Chaos enhancement in large-spin chains

Yael Lebel[1], Lea F. Santos[2] and Yevgeny Bar Lev[1]

1 Department of Physics, Ben-Gurion University of the Negev, Beer-Sheva 84105, Israel
2 Department of Physics, Yeshiva University, New York, New York 10016, USA

Abstract

We study the chaotic properties of a large-spin XXZ chain with onsite disorder and a small number of excitations above the fully polarized state. We show that while the classical limit, which is reached for large spins, is chaotic, enlarging the spin suppresses quantum chaos features. We examine ways to facilitate chaos by introducing additional terms to the Hamiltonian. Interestingly, perturbations that are diagonal in the basis of product states in the z-direction do not lead to significant enhancement of chaos, while off-diagonal perturbations restore chaoticity for large spins, so that only three excitations are required to achieve strong level repulsion and ergodic eigenstates.

Copyright Y. Lebel *et al*.
This work is licensed under the Creative Commons
Attribution 4.0 International License.
Published by the SciPost Foundation.

Received 06-04-2022
Accepted 22-05-2023
Published 21-07-2023
doi:10.21468/SciPostPhys.15.1.022

Check for updates

Contents

1 Introduction

Partially motivated by the Bohigas-Giannoni-Schmit conjecture [1, 2], quantum chaos was extensively studied in the 1980's and 1990's [3–5]. In the last ten years, the subject has seen a resurgence of interest due to its strong connection with several questions currently studied experimentally and theoretically, that include the issue of thermalization in isolated

many-body quantum systems [6–8], the problem of heating in driven systems [9–11], the difficulty to achieve many-body localization [12–15], and the fast scrambling of quantum information [16–20]. For systems with well-defined classical or semiclassical limits, quantum chaos refers to signatures found in the quantum domain, such as level statistics as in full random matrices [21], that indicate whether the classical system is chaotic in the sense of positive Lyapunov exponent and mixing. While this correspondence holds well for some systems with a small number of degrees of freedom, such as Sinai's billiard [1,2], it has recently been shown to be violated in triangular billiards [22] and quantum triangle maps [23]. As one moves to systems with many interacting particles, this issue gets even more complicated, since the classical limit is not always straightforward [24].

In this work, we investigate a one-dimensional system of many interacting spins described by the Heisenberg XXZ model with nearest-neighbor couplings and onsite disorder. We employ the term "quantum chaos" as a synonym for level statistics as in random matrices. When the total magnetization in the z-direction is close to zero, this model is chaotic for spin-1/2 [25], spin 1 [26, 27], and larger spins [28, 29]. For spin-1/2, the model has also been shown to demonstrate chaotic traits for as little as 3 or 4 excitations above a fully polarized state of spins [30,31] and even for a chain of only 3 spins-1/2 [32]. Here, we extend this analysis and examine the case of large-spin chains with a low number of excitations. In the semiclassical limit of a continuous spin, we verify that the system has a positive Lyapunov exponent. This might suggest that increasing the spin size would require even fewer excitations than in the case of spin-1/2 to reach the quantum chaotic regime. However, rather counterintuitively, the opposite takes place, larger spin takes us away from quantum chaos. We then try to remedy this problem by adding terms to the Hamiltonian. We show that chaos can be recovered with the inclusion of perturbations that are off-diagonal in the basis of product states in the z-direction, but the same does not happen for diagonal perturbations. With off-diagonal perturbations, quantum chaos can finally be reached with only 3 excitations.

2 The model

We consider the large-spin version of the XXZ model with onsite disorder and open boundaries described by the following Hamiltonian

$$\hat{H} = \frac{J_{xy}}{s(s+1)} \sum_{k=1}^{L-1} \left(\hat{S}_k^x \hat{S}_{k+1}^x + \hat{S}_k^y \hat{S}_{k+1}^y \right) + \frac{J_z}{s(s+1)} \sum_{k=1}^{L-1} \hat{S}_k^z \hat{S}_{k+1}^z + \frac{1}{\sqrt{s(s+1)}} \sum_{i=1}^{L} h_k \hat{S}_k^z , \qquad (1)$$

where $\hat{S}_k^\alpha$, with $\alpha = x, y, z$, stands for spin-s operators acting on a lattice site k with eigenvalues in $[-s, s]$. The parameter J_{xy} corresponds to the coupling strength in the xy plane and J_z stands for the strength of the interaction along the z-axis. To stay away from the isotropic point, $J_{xy} = J_z$, we choose $J_{xy} = 1$ and $J_z = 0.55$. The onsite disorder, where h_k is independent and uniformly distributed random numbers in the interval $[-W, W]$, is introduced to break spatial symmetries. We use a weak amplitude, $W = 0.5$, to avoid possible localization effects at higher disorder strength. For spin-1/2 and $W \sim J_{xy} \sim J_z$, model (1) is known to be chaotic [25, 33, 34]. The model conserves the total z-magnetization $\sum_k \hat{S}_k^z$, and through the work we consider almost fully polarized magnetization sectors with magnetization $-sL + N$. Here N is the number of excitations on top of the fully polarized state.

We write the Hamiltonian matrix in the basis corresponding to the eigenstates of S_k^z, that is, product states in the z-direction. This means that the terms involving the operators $\hat{S}_k^z$ are diagonal and those involving $\hat{S}_k^x \hat{S}_{k+1}^x + \hat{S}_k^y \hat{S}_{k+1}^y = \frac{1}{2} \left(\hat{S}_k^+ \hat{S}_{k+1}^- + \hat{S}_k^- \hat{S}_{k+1}^+ \right)$ are off-diagonal.

The effective Planck constant of the model is $\hbar_{eff} = I/\sqrt{s(s+1)}$, where I is the classical angular momentum which we set equal to 1. The semiclassical limit of Eq. (1) is obtained for very large spin numbers, $s \gg 1$. More precisely, to study the classical limit, it is convenient to normalize the spin operators, $\hat{\mathcal{S}}_k^\alpha = \hat{S}_k^\alpha/\sqrt{s(s+1)}$, which amounts to fixing the largest eigenvalue of the $\hat{\mathcal{S}}^2 = \sum_k \left(\hat{\mathcal{S}}_k^\alpha\right)^2$ operator to 1. Using the normalized spin operators, the quantum Hamiltonian is given by

$$\hat{H} = J_{xy}\sum_{k=1}^{L-1}\left(\hat{\mathcal{S}}_k^x\hat{\mathcal{S}}_{k+1}^x + \hat{\mathcal{S}}_k^y\hat{\mathcal{S}}_{k+1}^y\right) + J_z\sum_{k=1}^{L-1}\hat{\mathcal{S}}_k^z\hat{\mathcal{S}}_{k+1}^z + \sum_{i=1}^{L}h_k\hat{\mathcal{S}}_k^z\,, \tag{2}$$

where the commutation relations of the *normalized* spins follow directly from the standard commutation relations of the spin,

$$\left[\hat{\mathcal{S}}_k^\alpha, \hat{\mathcal{S}}_k^\beta\right] = i\frac{1}{\sqrt{s(s+1)}}\epsilon^{\alpha\beta\gamma}\hat{\mathcal{S}}_k^\gamma\,, \tag{3}$$

where $\epsilon^{\alpha\beta\gamma}$ is the Levi-Civita symbol. In the $s\to\infty$ limit the normalized spins commute, which corresponds to the classical limit. We can then replace the operators $\hat{\mathcal{S}}_k^\alpha$ by real numbers s_k^α, and obtain the classical version of the disordered XXZ model,

$$H_{cl} = J_{xy}\sum_{k=1}^{L-1}\left(s_k^x s_{k+1}^x + s_k^y s_{k+1}^y\right) + J_z\sum_{k=1}^{L-1}s_k^z s_{k+1}^z + \sum_{i=1}^{L}h_k s_k^z\,, \tag{4}$$

which represents classical interacting rotators $\vec{s}_k = \left(s_k^x, s_k^y, s_k^z\right)$ on a unit sphere. The classical system also conserves the total magnetization. We start by studying the chaotic properties of the model in the classical limit.

3 Classical chaos

To examine the chaotic properties of the classical Hamiltonian H_{cl} in Eq. (4), we examine the Lyapunov exponents starting from all the rotators pointing down in the z-direction, which corresponds to the lowest magnetization limit. The equations of motion of the rotators are obtained using Eq. (4) and Poisson brackets,

$$\frac{ds_k^\alpha}{dt} = \left\{H_{cl}, s_k^\alpha\right\}\,, \qquad \left\{s_k^\alpha, s_l^\beta\right\} = \delta_{kl}\epsilon^{\alpha\beta\gamma}s_k^\gamma\,, \tag{5}$$

which gives

$$\begin{aligned}
\frac{ds_k^x}{dt} &= -J_{xy}\left(s_{k+1}^y + s_{k-1}^y\right)s_k^z + \left[J_z\left(s_{k+1}^z + s_{k-1}^z\right) + h_k\right]s_k^y\,,\\
\frac{ds_k^y}{dt} &= J_{xy}\left(s_{k-1}^x + s_{k+1}^x\right)s_k^z - \left[J_z\left(s_{k+1}^z + s_{k-1}^z\right) + h_k\right]s_k^x\,,\\
\frac{ds_k^z}{dt} &= -J_{xy}\left[\left(s_{k-1}^x + s_{k+1}^x\right)s_k^y - \left(s_{k-1}^y + s_{k+1}^y\right)s_k^x\right]\,,
\end{aligned} \tag{6}$$

and can be compactly written as nonlinear Bloch equations,

$$\frac{d\vec{s}_k}{dt} = -\vec{b}_k\times\vec{s}_k\,, \tag{7}$$

with an effective magnetic field,

$$\vec{b}_k = \begin{pmatrix} J_{xy}\left(s^x_{k+1} + s^x_{k-1}\right) \\ J_{xy}\left(s^y_{k+1} + s^y_{k-1}\right) \\ h_k + J_z\left(s^z_{k+1} + s^z_{k-1}\right) \end{pmatrix}. \tag{8}$$

Since the equations conserve $s_k^2 = \vec{s}_k \cdot \vec{s}_k = 1$ for each rotator separately, the equation of one of the components of $\vec{s}$ is redundant and it is advantageous to use a numerical integration scheme which conserves all s_k^2 explicitly. One way to do this is to parametrize the orientation of the rotators on the unit sphere as $\vec{s}_k = (\sin\theta_k \cos\phi_k, \sin\theta_k \sin\phi_k, \cos\theta_k)$. This yields the following equations of motion for the angles,

$$\begin{aligned} \frac{d\phi_k}{dt} &= J_{xy} \sin\theta_{k-1} \cot\theta_k \left(\cos\phi_{k-1}\cos\phi_k + \sin\phi_{k-1}\sin\phi_k\right) \\ &\quad + J_{xy} \sin\theta_{k+1} \cot\theta_k \left(\cos\phi_{k+1}\cos\phi_k + \sin\phi_{k+1}\sin\phi_k\right) \\ &\quad - J_z\left(\cos\theta_{k+1} + \cos\theta_{k-1}\right) - h_k\,, \\ \frac{d\theta_k}{dt} &= J_{xy} \sin\theta_{k+1} \left(\cos\phi_{k+1}\sin\phi_k - \sin\phi_{k+1}\cos\phi_k\right) \\ &\quad + J_{xy} \sin\theta_{k-1} \left(\cos\phi_{k-1}\sin\phi_k - \sin\phi_{k-1}\cos\phi_k\right). \end{aligned} \tag{9}$$

To calculate the Lyapunov exponents of this system we initialize all of the rotors at angle θ from the z axis. Angles $\theta \approx 0$ correspond to the low magnetization setting considered in this work. For each disorder realization we initiate the angles ϕ_k in the xy plane randomly in $[-\pi, \pi]$, and integrate the equations of motion. The maximal Lyapunov exponent is calculated with the algorithm proposed in Ref. [35], which is based on finding the rate of growth of the fastest growing tangent space vector. The process involves selecting a starting distance, between two phase space trajectories. This distance is allowed to diverge over a short period of time, before being reset back to its initial value. The procedure is repeated, and the largest Lyapunov exponent is determined from a sum of divergences [35].

We use a chain of 50 spins to calculate the Lyapunov exponents and integrate Eq. (9) using the LSODA method described in Ref. [36] with time steps chosen optimally by the algorithm.

In Fig. 1 for each angle θ we present the largest Lyapunov exponents computed for 100 different realizations of disorder and initial conditions, ϕ_k. We do not average the data to show the spread of the exponents. It can be seen that even for low values of θ, which is equivalent to a low number of excitations in the quantum limit, the largest Lyapunov exponent is positive, indicating that the classical limit is chaotic.

4 Quantum chaos

After establishing that the classical limit of our model in Eq. (4) is chaotic at low magnetization, we proceed to examine whether the quantum Hamiltonian in Eq. (1) exhibits properties associated with quantum chaos. These properties include correlated eigenvalues, as in random matrix theory, and eigenstates that away from the edges of the spectrum are close to the eigenstates of full random matrices, that is, their components are nearly independent real random numbers from a Gaussian distribution satisfying the normalization condition [6, 7]. The onset of these almost random vectors in many-body quantum systems results in normal distributions of the off-diagonal elements of local observables [37–43], which is one of the features of the eigenstate thermalization hypothesis (ETH) [27, 44–52].

Needless to say, realistic many-body quantum models differ from full random matrices (see Ref. [7] and references therein, and for newer discussions in the context of ETH, see [53–

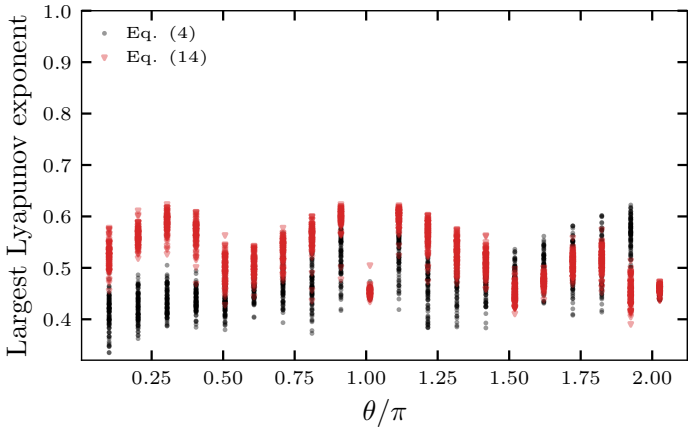

Figure 1: Largest Lyapunov exponents as a function of θ/π. Each point corresponds to a different realization of disorder and the angles of the rotors in the xy-plane, ϕ_k. The black circles correspond to the largest Lyapunov exponent of the model in Eq. (4), while the red triangles correspond to the largest Lyapunov exponent of the model in Eq. (14) with additional nonlinear terms. A chain of $L = 50$ is considered for these simulations.

55]). One looks for properties similar to those of full random matrices, however, correlations are always present among the elements of the Hamiltonian matrix of real systems. These correlations then affect the structure of the eigenstates and the results for the observables. In this work, we analyze how the properties of our system further depart from those of random matrices as we increase the spin size s.

Our analysis of quantum chaos focuses on level statistics and the off-diagonal ETH. It is done for the subspace with total z-magnetization equal to $-sL+N$, where N is a fixed number of excitations.

To study the level statistics, we use the so called r-metric [56–58],

$$r_\alpha = \min\left(\frac{\delta_\alpha}{\delta_{\alpha-1}}, \frac{\delta_{\alpha-1}}{\delta_\alpha}\right), \tag{10}$$

where $\delta_\alpha = E_{\alpha+1} - E_\alpha$ is the spacing between the neighboring eigenvalues of the Hamiltonian. The r-metric captures short-range correlations among the energy levels. For an integrable system with Poissonian level spacing distribution, the average of r_α over the spectrum gives $r_{\text{Poisson}} \approx 0.39$, while for chaotic systems $r_{\text{GOE}} \approx 0.53$ [57]. The latter is the value obtained for full random matrices from Gaussian orthogonal ensembles (GOE) [57].

In Fig. 2 we plot the average of the r-metric, $\langle r \rangle$, for four different spin sizes as a function of the number N of excitations in the system. We repeat our calculations for chain lengths ranging from 10 to 38 sites (darker colors indicate larger chains). Surprisingly, while the classical limit of this model is chaotic, as shown in the previous section, for larger spin sizes, *more* excitations are required to reach signatures of chaos in the quantum domain. Similarly to the spin-1/2 model studied in Refs. [30, 31], the system with spin 1 is fairly chaotic for $N = 3$ and 4, as seen in Figs. 2 (a)-(b), but $\langle r \rangle$ for the spin-4 model does not reach r_{GOE} for the system sizes considered, as evident in Fig. 2 (d). For a fixed system size and a fixed number of excitations, the r-metric in Fig. 2 indicates that a system with a larger spin presents a weaker degree of chaos than its counterpart with a smaller spin.

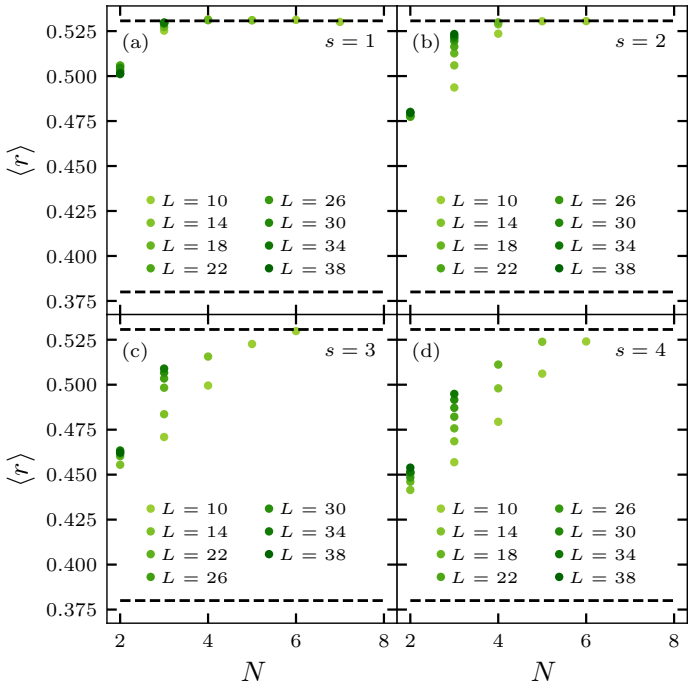

Figure 2: Average of the r-metric for four different spin sizes, $s = 1, 2, 3, 4$, as a function of the number of excitations N and various system sizes. Darker circles represent larger chain sizes (see legends). In the calculations of this metric, the top and bottom 15% of the eigenvalues are omitted. The dashed horizontal lines stand for $r_{\text{Poisson}} = 0.39$ and $r_{\text{GOE}} = 0.53$. The average is performed over 250 disorder realizations.

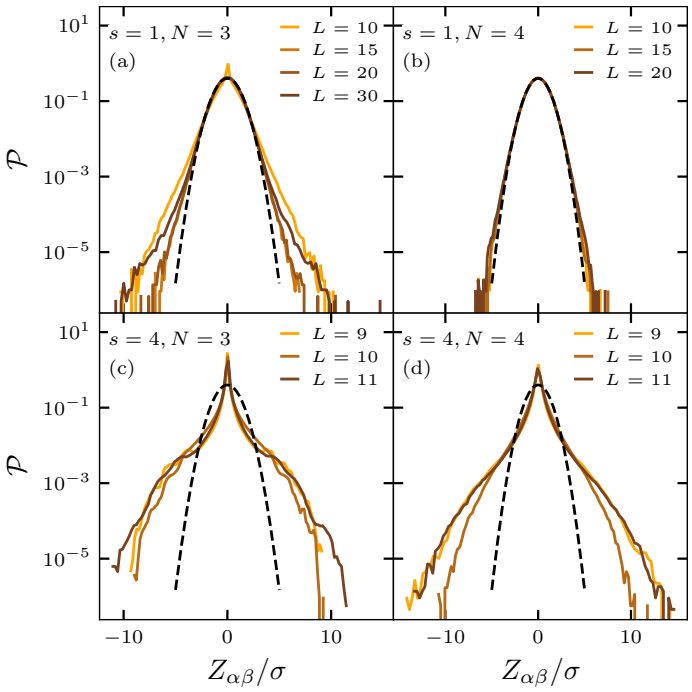

Figure 3: Distributions of the off-diagonal elements of the $\hat{S}^z_{L/2}$ operator for spin 1 (top row) and spin 4 (bottom row) and varying system sizes. Left column corresponds to $N = 3$ excitations and right column to $N = 4$ excitations. We use 250 eigenstates in the middle of the spectrum to compute the off-diagonal elements, and normalize the distributions to have unit variance. The dashed black line shows a Gaussian distribution with unit variance.

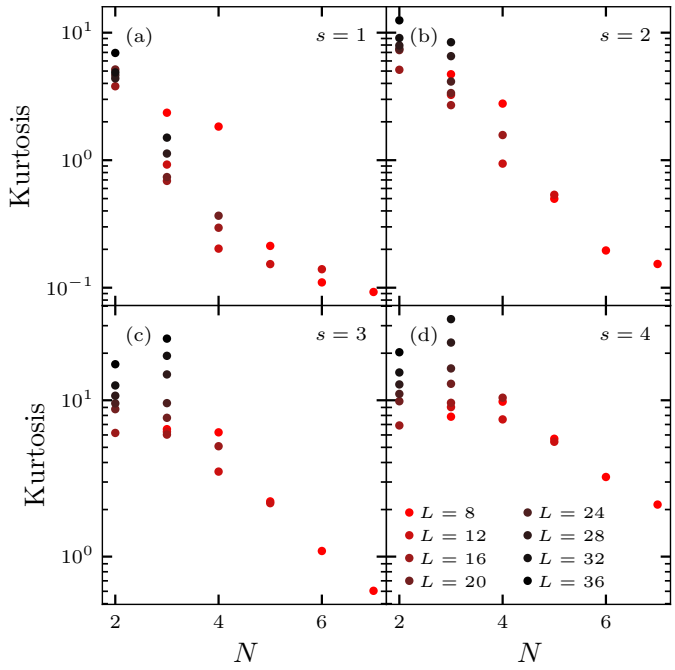

Figure 4: Kurtosis of the distributions of the off-diagonal elements of the $\hat{S}^z_{L/2}$ operator for four different spin sizes, $s = 1, 2, 3, 4$, as a function of the number of excitations N and various system sizes. Darker circles represent larger chain sizes (see legends). In the calculations of the kurtosis we used 250 eigenstates from the middle of the spectrum. For a chaotic system the kurtosis is supposed to be zero.

To better understand why the degree of quantum chaos decreases as the spin is enlarged, we resort to the analysis of the distribution of the off-diagonal elements of the local magnetization, $\hat{S}^z_{L/2}$. For this purpose we take 250 states from the middle of the spectrum and compute the matrix elements $Z_{\alpha\beta} \equiv \langle\alpha|\hat{S}^z_{L/2}|\beta\rangle$ where $|\alpha\rangle$ and $|\beta\rangle$ are two different eigenstates. Since the variance of the distribution decreases with the Hilbert space dimension $\mathcal{D}$ [49], we normalize the distribution by dividing $Z_{\alpha\beta}$ by its standard deviation,

$$\sigma = \sqrt{\left\langle Z^2_{\alpha\beta}\right\rangle - \left\langle Z_{\alpha\beta}\right\rangle^2}\,, \tag{11}$$

where $\langle . \rangle$ indicates the average over all different pairs of eigenstates $|\alpha\rangle$ and $|\beta\rangle$ that we retain. The resulting distributions for $s = 1$, 4 and $N = 3$,4 can be seen in Fig. 3. The distributions for the spin-1 case in Figs. 3 (a)-(b) are very close to Gaussian (dashed black line) for both $N = 3$ [Fig. 3 (a)] and $N = 4$ [Fig. 3 (b)] excitations. However, the spin-4 distributions depicted in Fig. 3 (c)-(d) are strongly peaked around zero. To quantify how close the distributions are to a Gaussian, we calculate their normalized kurtosis,

$$\kappa = \frac{\langle O^4_{\alpha\beta}\rangle - \langle O_{\alpha\beta}\rangle^4}{\sigma^4} - 3\,, \tag{12}$$

which is equal to 0 for a Gaussian distribution. Figure 4 shows the kurtosis of the distributions for $s = 1, 2, 3$ and 4 as a function of the number of excitations N for different system sizes. For $s = 3$ and 4 [Figs. 4 (c)-(d)] the dependence of the kurtosis on the number of excitations is non-monotonic around $N = 2, 3$. For $s = 4$ in Fig. 4 (d), the kurtosis only decreases when $N > 4$, and much slower than for $s = 1, 2$ in Figs. 4 (a)-(b). Notice that the scale in the y-axis for $s = 1, 2$ in Figs. 4 (a)-(b) is not the same as for $s = 3, 4$ in Figs. 4 (c)-(d). These results

confirm that larger spins require more excitations to reach the chaotic regime. Note that the situation does not improve with system size, since for larger L, the kurtosis actually moves further away from zero, specially for $s = 3, 4$ around $N = 2, 3$.

In the following section we consider ways to restore quantum chaos in large-spin chains by perturbing the original model.

5 Enhancing quantum chaos

We consider two ways to improve the chaotic properties of the finite, large-spin system in Eq. (1) by modifying its Hamiltonian. The first mechanism consisting of adding properly normalized nonlinear magnetization terms to the Hamiltonian,

$$H_1 = H + \frac{\alpha}{s(s+1)} \sum_k \left(\hat{S}_k^z\right)^2 + \frac{\mu}{(s(s+1))^{3/2}} \sum_k \left(\hat{S}_k^z\right)^3 , \tag{13}$$

where $\alpha = 0.87, \mu = 0.91$. The new term in Eq. (13) corresponds to a diagonal perturbation to the Hamiltonian (1) written in the basis of product states in the z-direction.

The classical limit of this model is

$$H_1^{cl} = H_{cl} + \alpha \sum_k \left(s_k^z\right)^2 + \mu \sum_k \left(s_k^z\right)^3 . \tag{14}$$

In Fig. 1, we present the maximal Lyapunov exponents of this model with red points and verify that they closely follow the Lyapunov exponents of the classical disordered XXZ model in Eq. (4). We note that the addition of these terms slightly increases the Lyapunov exponents.

The second quantum chaos enhancement mechanism that we consider is via an off-diagonal perturbation of the form,

$$H_2 = H_1 + \sum_{k=1}^{L-1} \sum_{n=2}^{s} \frac{J_{xy}}{s^n (s+1)^n} \left[\left(\hat{S}_k^+ \hat{S}_{k+1}^-\right)^n + \left(\hat{S}_{k+1}^+ \hat{S}_k^-\right)^n \right] . \tag{15}$$

The added terms move n-excitations between neighboring sites with $2 \leq n \leq s$. While the classical limit of this model is well defined, the derivation of its Hamiltonian in a closed form is cumbersome, because the sum over n of the nonlinear ladder operators has to be computed explicitly, so we do not show it here.

The results for the Hamiltonians in Eq. (13) and Eq. (15) show a systematic improvement for all considered quantum chaos metrics when compared to the disordered XXZ model in Eq. (1). Figure 5 shows the average r-metric of all three models computed for spin 1 [Figs. 5 (a)-(b)] and spin 4 [Figs. 5 (c)-(d)] as a function of the Hilbert space dimension, $\mathcal{D}$. The spin-1 case is already fairly chaotic for the Hamiltonian (1), so the addition of the new terms in Eq. (13) and Eq. (15) do not affect the values of $\langle r \rangle$. However, for spin 4, adding the nonlinear magnetization terms in Eq. (13) dramatically improves the degree of quantum chaos for both $N = 3$ and 4. The addition of the nonlinear ladder operators in Eq. (15) is even more effective and leads to strong level repulsion for as few as 3 excitations, making the results analogous to the case of spin-1/2 studied in Ref. [31]. This significant enhancement of the degree of quantum chaos is corroborated by the other chaotic metrics considered in this work, namely the distributions of off-diagonal observables and the kurtosis of these distributions (not shown).

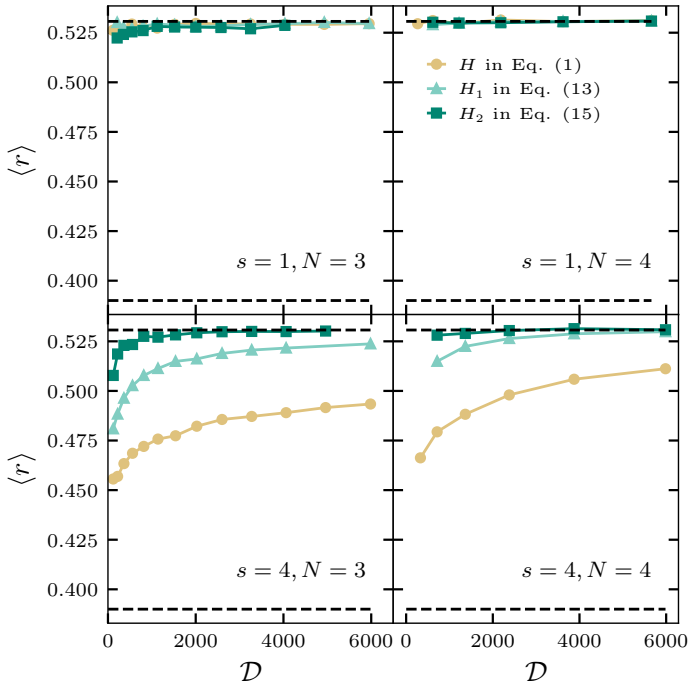

Figure 5: Averaged r-metric as a function of the Hilbert space dimension $\mathcal{D}$ for spin-1 models (top row) and spin-4 models (bottom row). The left column shows $N = 3$ excitations and the right column shows $N = 4$ excitations. Circles correspond to the disordered XXZ model in Eq. (1), triangles to the model in Eq. (13), and squares to the model in Eq. (15). The dashed horizontal lines stand for $r_{\text{Poisson}} = 0.39$ and $r_{\text{GOE}} = 0.5307$.

6 Large-spin limit

In this section, we investigate whether the chaos enhancements that we proposed in Sec. 5 survive in the limit of large-spins. The system remains restricted to the low-magnetization sector with $\sum_k S^z_k = -sL + N$. In this sector, the operator norm of the diagonal terms in Hamiltonians (1), (13) and (15) asymptotically, do not depend on s. On the other hand, the

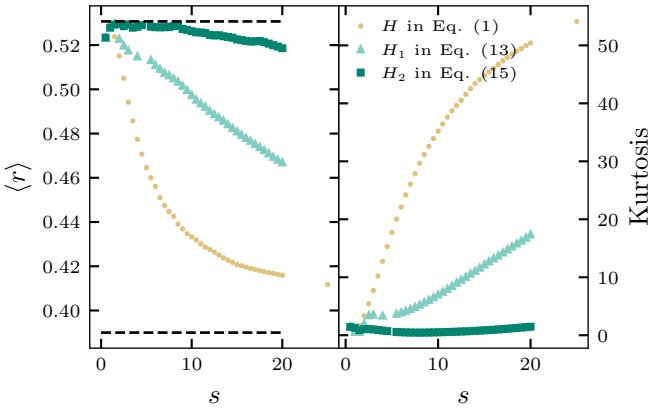

Figure 6: Average r-metric (left) and kurtosis (right) as a function of spin for $N = 3$. Circles correspond to the disordered XXZ model (1), triangles to model (13), and squares to model (15). The dashed horizontal lines stand for $r_{\text{Poisson}} = 0.39$ and $r_{\text{GOE}} = 0.5307$.

operator norm of the off-diagonal terms decrease with s as N/s.

In the classical limit, despite the small energy contribution of the terms containing spin projections on the xy-plane, the Lyapunov exponent remains positive, as shown in Fig. 1. In the quantum domain, chaos is only robust for the Hamiltonian in Eq. (15). This is shown in Fig. 6, where we plot the r-statistics for spins up to $s = 20$ and $N = 3$. The unperturbed Hamiltonian in Eq. (1) and the diagonally perturbed Hamiltonian in Eq. (13) become increasingly non-chaotic for larger spins. On the other hand, the off-diagonally perturbed Hamiltonian in Eq. (15) stays chaotic, with only a slight decrease in the chaotic properties.

7 Discussion

The driving question of this work is whether increasing the spin size of a one-dimensional spin model can reduce the number of spin excitations needed to achieve quantum chaos. For this purpose we studied the large spin limit of a disordered XXZ chain. For a single spin-1/2 excitation this model is integrable and localized via the Anderson localization mechanism, while at zero z-magnetization and sufficiently low disorder it is chaotic. In previous studies of spin-1/2 chains, it was established that at least 3 spin excitations are required to achieve quantum chaos [30, 31]. In the present work, by considering chaotic metrics based on both the eigenvalues and the eigenstates, we found that, although the classical limit of the disordered XXZ chain is chaotic for very low magnetization, the large spin version of the quantum XXZ model, surprisingly, shows significantly reduced chaotic behavior, compared to its spin-1/2 counterpart. We analyzed two ways of enhancing quantum chaotic behavior: by the introduction of diagonal and off-diagonal perturbations to the Hamiltonian. Interestingly, while the diagonal perturbation enhances chaos only slightly, off-diagonal perturbation allows for the onset of quantum chaos with only $N = 3$ excitations. In addition, we showed that while the unperturbed and diagonally perturbed Hamiltonian show diminishing quantum chaos properties in the large-spin limit, the off-diagonally perturbed Hamiltonian stays chaotic for spins as large as $s = 20$. An interesting question, which our study raises, is which types of off-diagonal perturbations lead to quantum chaotic behavior in the large-spin limit? More broadly, our study suggests that care should be taken in considering large-spin limits of quantum models and that classical and quantum chaos might not be so tightly bound.

Acknowledgments

Funding information This research was supported by a grant from the United States-Israel Binational Foundation (BSF, Grant No. 2019644), Jerusalem, Israel, and the United States National Science Foundation (NSF, Grant No. DMR−1936006), and by the Israel Science Foundation (grants No. 527/19 and 218/19).

References

[1] G. Casati, F. Valz-Gris and I. Guarnieri, *On the connection between quantization of non-integrable systems and statistical theory of spectra*, Lett. Nuovo Cimento **28**, 279 (1980), doi:10.1007/bf02798790.

[2] O. Bohigas, M. J. Giannoni and C. Schmit, *Characterization of chaotic quantum spectra and universality of level fluctuation laws*, Phys. Rev. Lett. **52**, 1 (1984),

doi:10.1103/physrevlett.52.1.

[3] H.-J. Stockmann, *Quantum chaos*, Cambridge University Press, Cambridge, UK, ISBN 9780511524622 (2007), doi:10.1017/CBO9780511524622.

[4] F. Haake, *Quantum signatures of chaos*, Springer Berlin, Heidelberg, Germany, ISBN 9783642054280 (2001), doi:10.1007/978-3-642-05428-0.

[5] L. E. Reichl, *The transition to chaos*, Springer, New York, USA, ISBN 9781475743524 (1994), doi:10.1007/978-1-4757-4352-4.

[6] V. Zelevinsky, B. A. Brown, N. Frazier and M. Horoi, *The nuclear shell model as a testing ground for many-body quantum chaos*, Phys. Rep. **276**, 85 (1996), doi:10.1016/s0370-1573(96)00007-5.

[7] F. Borgonovi, F. M. Izrailev, L. F. Santos and V. G. Zelevinsky, *Quantum chaos and thermalization in isolated systems of interacting particles*, Phys. Rep. **626**, 1 (2016), doi:10.1016/j.physrep.2016.02.005.

[8] L. D'Alessio, Y. Kafri, A. Polkovnikov and M. Rigol, *From quantum chaos and eigenstate thermalization to statistical mechanics and thermodynamics*, Adv. Phys. **65**, 239 (2016), doi:10.1080/00018732.2016.1198134.

[9] L. D'Alessio and M. Rigol, *Long-time behavior of isolated periodically driven interacting lattice systems*, Phys. Rev. X **4**, 041048 (2014), doi:10.1103/PhysRevX.4.041048.

[10] A. Lazarides, A. Das and R. Moessner, *Fate of many-body localization under periodic driving*, Phys. Rev. Lett. **115**, 030402 (2015), doi:10.1103/PhysRevLett.115.030402.

[11] D. S. Bhakuni, L. F. Santos and Y. Bar Lev, *Suppression of heating by long-range interactions in periodically driven spin chains*, Phys. Rev. B **104**, L140301 (2021), doi:10.1103/PhysRevB.104.L140301.

[12] R. Nandkishore and D. A. Huse, *Many-body localization and thermalization in quantum statistical mechanics*, Annu. Rev. Condens. Matter Phys. **6**, 15 (2015), doi:10.1146/annurev-conmatphys-031214-014726.

[13] D. A. Abanin and Z. Papić, *Recent progress in many-body localization*, Ann. Phys. **529**, 1700169 (2017), doi:10.1002/andp.201700169.

[14] K. Agarwal, E. Altman, E. Demler, S. Gopalakrishnan, D. A. Huse and M. Knap, *Rare-region effects and dynamics near the many-body localization transition*, Ann. Phys. **529**, 1600326 (2017), doi:10.1002/andp.201600326.

[15] D. J. Luitz and Y. Bar Lev, *The ergodic side of the many-body localization transition*, Ann. Phys. **529**, 1600350 (2017), doi:10.1002/andp.201600350.

[16] B. Swingle, G. Bentsen, M. Schleier-Smith and P. Hayden, *Measuring the scrambling of quantum information*, Phys. Rev. A **94**, 040302 (2016), doi:10.1103/PhysRevA.94.040302.

[17] M. Gärttner, J. G. Bohnet, A. Safavi-Naini, M. L. Wall, J. J. Bollinger and A. M. Rey, *Measuring out-of-time-order correlations and multiple quantum spectra in a trapped-ion quantum magnet*, Nat. Phys. **13**, 781 (2017), doi:10.1038/nphys4119.

[18] F. Borgonovi, F. M. Izrailev and L. F. Santos, *Exponentially fast dynamics of chaotic many-body systems*, Phys. Rev. E **99**, 010101 (2019), doi:10.1103/physreve.99.010101.

[19] C. M. Sánchez, A. K. Chattah, K. X. Wei, L. Buljubasich, P. Cappellaro and H. M. Pastawski, *Perturbation independent decay of the Loschmidt echo in a many-body system*, Phys. Rev. Lett. **124**, 030601 (2020), doi:10.1103/PhysRevLett.124.030601.

[20] M. Niknam, L. F. Santos and D. G. Cory, *Sensitivity of quantum information to environment perturbations measured with a nonlocal out-of-time-order correlation function*, Phys. Rev. Res. **2**, 013200 (2020), doi:10.1103/PhysRevResearch.2.013200.

[21] T. Guhr, A. Müller-Groeling and H. A. Weidenmüller, *Random-matrix theories in quantum physics: Common concepts*, Phys. Rep. **299**, 189 (1998), doi:10.1016/S0370-1573(97)00088-4.

[22] Č. Lozej, G. Casati and T. Prosen, *Quantum chaos in triangular billiards*, Phys. Rev. Res. **4**, 013138 (2022), doi:10.1103/physrevresearch.4.013138.

[23] J. Wang, G. Benenti, G. Casati and W.-G. Wang, *Statistical and dynamical properties of the quantum triangle map*, J. Phys. A: Math. Theor. **55**, 234002 (2022), doi:10.1088/1751-8121/ac6a93.

[24] M. Akila, D. Waltner, B. Gutkin, P. Braun and T. Guhr, *Semiclassical identification of periodic orbits in a quantum many-body system*, Phys. Rev. Lett. **118**, 164101 (2017), doi:10.1103/PhysRevLett.118.164101.

[25] Y. Avishai, J. Richert and R. Berkovits, *Level statistics in a Heisenberg chain with random magnetic field*, Phys. Rev. B **66**, 052416 (2002), doi:10.1103/PhysRevB.66.052416.

[26] J. Richter, N. Casper, W. Brenig and R. Steinigeweg, *Magnetization dynamics in clean and disordered spin-1 XXZ chains*, Phys. Rev. B **100**, 144423 (2019), doi:10.1103/physrevb.100.144423.

[27] L. F. Santos, F. Pérez-Bernal and E. J. Torres-Herrera, *Speck of chaos*, Phys. Rev. Res. **2**, 043034 (2020), doi:10.1103/physrevresearch.2.043034.

[28] A. S. de Wijn, B. Hess and B. V. Fine, *Largest Lyapunov exponents for lattices of interacting classical spins*, Phys. Rev. Lett. **109**, 034101 (2012), doi:10.1103/physrevlett.109.034101.

[29] T. A. Elsayed and B. V. Fine, *Sensitivity to small perturbations in systems of large quantum spins*, Phys. Scr. 014011 (2015), doi:10.1088/0031-8949/2015/t165/014011.

[30] M. Schiulaz, M. Távora and L. F. Santos, *From few- to many-body quantum systems*, Quantum Sci. Technol. **3**, 044006 (2018), doi:10.1088/2058-9565/aad913.

[31] G. Zisling, L. Santos and Y. Bar Lev, *How many particles make up a chaotic many-body quantum system?*, SciPost Phys. **10**, 088 (2021), doi:10.21468/SciPostPhys.10.4.088.

[32] N. Mirkin and D. Wisniacki, *Quantum chaos, equilibration, and control in extremely short spin chains*, Phys. Rev. E **103**, L020201 (2021), doi:10.1103/PhysRevE.103.L020201.

[33] L. F. Santos, G. Rigolin and C. O. Escobar, *Entanglement versus chaos in disordered spin chains*, Phys. Rev. A **69**, 042304 (2004), doi:10.1103/physreva.69.042304.

[34] L. F. Santos, *Integrability of a disordered Heisenberg spin-1/2 chain*, J. Phys. A: Math. Gen. **37**, 4723 (2004), doi:10.1088/0305-4470/37/17/004.

[35] T. A. Elsayed, B. Hess and B. V. Fine, *Signatures of chaos in time series generated by many-spin systems at high temperatures*, Phys. Rev. E **90**, 022910 (2014), doi:10.1103/PhysRevE.90.022910.

[36] L. Petzold, *Automatic selection of methods for solving stiff and nonstiff systems of ordinary differential equations*, SIAM J. Sci. Stat. Comput. **4**, 1 (1983), doi:10.1137/0904010.

[37] P. Pechukas, *Distribution of energy eigenvalues in the irregular spectrum*, Phys. Rev. Lett. **51**, 943 (1983), doi:10.1103/PhysRevLett.51.943.

[38] P. Pechukas, *Remarks on "quantum chaos"*, J. Phys. Chem. **88**, 4823 (1984), doi:10.1021/j150665a006.

[39] A. Peres, *Ergodicity and mixing in quantum theory. I*, Phys. Rev. A **30**, 504 (1984), doi:10.1103/PhysRevA.30.504.

[40] A. Peres, *Stability of quantum motion in chaotic and regular systems*, Phys. Rev. A **30**, 1610 (1984), doi:10.1103/PhysRevA.30.1610.

[41] M. Feingold, N. Moiseyev and A. Peres, *Ergodicity and mixing in quantum theory. II*, Phys. Rev. A **30**, 509 (1984), doi:10.1103/PhysRevA.30.509.

[42] M. Feingold, N. Moiseyev and A. Peres, *Classical limit of quantum chaos*, Chem. Phys. Lett. **117**, 344 (1985), doi:10.1016/0009-2614(85)85241-6.

[43] M. Feingold and A. Peres, *Distribution of matrix elements of chaotic systems*, Phys. Rev. A **34**, 591 (1986), doi:10.1103/PhysRevA.34.591.

[44] J. M. Deutsch, *Quantum statistical mechanics in a closed system*, Phys. Rev. A **43**, 2046 (1991), doi:10.1103/PhysRevA.43.2046.

[45] M. Srednicki, *Chaos and quantum thermalization*, Phys. Rev. E **50**, 888 (1994), doi:10.1103/PhysRevE.50.888.

[46] M. Srednicki, *Thermal fluctuations in quantized chaotic systems*, J. Phys. A: Math. Gen. **29**, L75 (1996), doi:10.1088/0305-4470/29/4/003.

[47] M. Srednicki, *The approach to thermal equilibrium in quantized chaotic systems*, J. Phys. A: Math. Gen. **32**, 1163 (1999), doi:10.1088/0305-4470/32/7/007.

[48] M. Rigol, V. Dunjko and M. Olshanii, *Thermalization and its mechanism for generic isolated quantum systems*, Nature **452**, 854 (2008), doi:10.1038/nature06838.

[49] W. Beugeling, R. Moessner and M. Haque, *Off-diagonal matrix elements of local operators in many-body quantum systems*, Phys. Rev. E **91**, 012144 (2015), doi:10.1103/PhysRevE.91.012144.

[50] T. LeBlond, K. Mallayya, L. Vidmar and M. Rigol, *Entanglement and matrix elements of observables in interacting integrable systems*, Phys. Rev. E **100**, 062134 (2019), doi:10.1103/PhysRevE.100.062134.

[51] I. M. Khaymovich, M. Haque and P. A. McClarty, *Eigenstate thermalization, random matrix theory, and behemoths*, Phys. Rev. Lett. **122**, 070601 (2019), doi:10.1103/physrevlett.122.070601.

[52] P. Łydżba, Y. Zhang, M. Rigol and L. Vidmar, *Single-particle eigenstate thermalization in quantum-chaotic quadratic Hamiltonians*, Phys. Rev. B **104**, 214203 (2021), doi:10.1103/physrevb.104.214203.

[53] L. Foini and J. Kurchan, *Eigenstate thermalization hypothesis and out of time order correlators*, Phys. Rev. E **99**, 042139 (2019), doi:10.1103/PhysRevE.99.042139.

[54] J. Richter, A. Dymarsky, R. Steinigeweg and J. Gemmer, *Eigenstate thermalization hypothesis beyond standard indicators: Emergence of random-matrix behavior at small frequencies*, Phys. Rev. E **102**, 042127 (2020), doi:10.1103/PhysRevE.102.042127.

[55] M. Brenes, S. Pappalardi, M. T. Mitchison, J. Goold and A. Silva, *Out-of-time-order correlations and the fine structure of eigenstate thermalization*, Phys. Rev. E **104**, 034120 (2021), doi:10.1103/PhysRevE.104.034120.

[56] V. Oganesyan and D. A. Huse, *Localization of interacting fermions at high temperature*, Phys. Rev. B **75**, 155111 (2007), doi:10.1103/PhysRevB.75.155111.

[57] Y. Y. Atas, E. Bogomolny, O. Giraud and G. Roux, *Distribution of the ratio of consecutive level spacings in random matrix ensembles*, Phys. Rev. Lett. **110**, 084101 (2013), doi:10.1103/PhysRevLett.110.084101.

[58] Á. L. Corps and A. Relaño, *Distribution of the ratio of consecutive level spacings for different symmetries and degrees of chaos*, Phys. Rev. E **101**, 022222 (2020), doi:10.1103/PhysRevE.101.022222.